Reports of Biochemistry & Molecular Biology
Vol.12, No.1, Apr 2023

Original article

www.RBMB.net

Anti-Cancer Effect of *Dorema Ammoniacum Gum* by Targeting Metabolic Reprogramming by Regulating *APC*, *P53*, *KRAS* Gene Expression in HT-29 Human Colon Cancer Cells

Elham Ghodousi-Dehnavi[1], Mohammad Arjmand*[2], Ziba Akbari[2], Mansour Aminzadeh[2], Reza Haji Hosseini[1]

Abstract

Background: Colorectal cancer is a heterogeneous disease that leads to metabolic disorders due to multiple upstream genetic and molecular changes and interactions. The development of new therapies, especially herbal medicines, has received much global attention. *Dorema ammoniacum* is a medicinal plant. Its gum is used in healing known ailments. Studying metabolome profiles based on nuclear magnetic resonance 1HNMR as a non-invasive and reproducible tool can identify metabolic changes as a reflection of intracellular fluxes, especially in drug responses.

This study aimed to investigate the anti-cancer effects of different gum extracts on metabolic changes and their impact on gene expression in HT-29 cell.

Methods: Extraction of *Dorema ammoniacum* gum with hexane, chloroform, and dichloromethane organic solvents was performed. Cell inhibition growth percentage and IC_{50} were assessed. Following treating the cells with dichloromethane extract, *p53, APC,* and *KRAS* gene expression were determined. 1HNMR spectroscopy was conducted. Eventually, systems biology software tools interpreted combined metabolites and genes simultaneously.

Results: The lowest determined IC_{50} concentration was related to dichloromethane solvent, and the highest was hexane and chloroform. The expression of the *KRAS* oncogene gene decreased significantly after treatment with dichloromethane extract compared to the control group, and the expression of tumor suppressor gene *p53* and *APC* increased significantly. Most gene-altered convergent metabolic phenotypes.

Conclusions: This study's results indicate that the dichloromethane solvent of *Dorema ammoniacum* gum exhibits its antitumor properties by altering the expression of genes involved in HT-29 cells and the consequent change in downstream metabolic reprogramming.

Keywords: *APC,* HT-29 cell, *KRAS*, Metabolomics, Nuclear Magnetic Resonance, *P53*.

[DOI: 10.61186/rbmb.12.1.127]

Introduction

Colorectal cancer is the third most considerable cancer incidence and the second leading cause of cancer mortality worldwide, with the highest prevalence in women (1). Colorectal cancer starts from benign adenosine polyps and progresses to dysplasia, an advanced, invasive adenoma known as multistage tumorigenesis. The multistage tumorigenesis is due to multiple genetic and molecular mechanisms proposed in the cell biochemical pathway and sequential genetic changes such as mutations in the early stages of *APC* and mutations in the *KRAS* oncogene gene and *p53* tumor suppressor in later stages

1: Department of Biology, Faculty of Science, Payame Noor University, Tehran, Iran.
2: Metabolomics Lab. Department of Biochemistry, Pasteur Institute of Iran, Pasteur Avenue, Tehran, Iran.
***Corresponding author: Mohammad Arjmand; Tel: +98 21 64112140; E-mail: arjmand1@yahoo.com.**
Received: 16 Jan, 2023; Accepted: 16 Feb, 2023

(2). These ultimately cause fundamental changes in cell biology, disruption of the differentiation and maintenance of genomic DNA, the onset and increase and accumulation of *CRC* progression factors, and increased cell proliferation. It is also well known that about 10-80% of the dominant mutations in colorectal cancer are caused by mutations in genes such as *APC, p53, and KRAS* (3, 4). The genus *Dorema* ammoniacum *D. Don* of the *Apiaceae* family genus *Dorema*, with seven species in Iran's flora, is a medicinal plant known in traditional Iranian medicine. Gum resin secreted from damaged stems and roots is used as an expectorant, stimulant, and antispasmodic to eliminate gastrointestinal disorders and anti-inflammatory skin to treat asthma, bronchitis, and cataracts (5, 6). Numerous biological and medicinal activities have also been described, including antibacterial, antifungal, expectorant, anticonvulsant, antimicrobial, antioxidant, and vasodilator acetylcholinesterase inhibitors (7). This study aimed to evaluate the anti-cancer properties of *Dorema ammoniacum* gum extract on the metabolome profile changes of HT-29 cells through its effect on genes' expression in the carcinogenicity of *p53 KRAS* and *APC*.

Materials and Methods

Dorema ammoniacum gum extraction

Dorema ammoniacum gum was obtained from the Kashan region, Iran. A voucher specimen was deposited in the Tehran university's Herbarium center (No. Pmp1836). 20 g of powdered gum was dissolved separately in 200 ml of organic solvents with different polarities, including chloroform, hexane, and chloromethane. They were placed in Soxhlet extraction thimbles, following extraction at 45 °C for 2 hours. Later, the solvent was evaporated at 40 °C by a rotary evaporated apparatus under vacuum pressure. All extracts were freeze-dried, and the amount of dry brown extracts obtained from chloroform, hexane, and dichloromethane solvents were 9.64, 10.94, and 8.6 grams, respectively. They were kept at -20 °C until used for the assay (8, 9).

Cell culture

The colorectal cancer cell, line H-29 (NCBI code C154 and ATCC number HTB-38), was purchased from the Pasteur Institute of Iran, cultured in DMEM medium containing 10% FBS (bovine fetal serum), 100 µg/ml streptomycin, and 100 U/ml penicillin. The tissue flask was incubated at 37 °C, 5% CO2, with 95% humidity. The cells were often karyotyped and tested for any contamination.

Cytotoxicity assay

In each 96-cell plate well, 10^4 cells were cultured. After 24 hours, 50 µl of various concentrations of chloroform, hexane, and dichloromethane solvent extracts of *Dorema* ammoniacum gum (0, 50, 100, 200, 300, 400, 500, and 600 µg/ml) were added and incubated for 48 hours. Also, untreated cells were used as a negative control, and the blank contained DMEM medium alone. 20 µl of MTT reagent (3-(4,5-dimethylthiazol-2-yl)-2,5-diphenyl-2H-tetrazolium bromide) was added to each well and incubated for 4 hours. The supernatant was aspirated from each well, then 150 µl of (Dimethyl sulfoxide) DMSO was added, and the plate was shaken for 15 minutes. Also, absorbance was measured for each well at 570 nm and reference length wave at 630 nm. The absorbance of untreated cells is considered 100%. All extract and control were assayed in triplicate in three independent experiments. The cytotoxic effects of the extracts were assessed in terms of growth inhibition percentage and expressed as IC_{50}, which is the concentration of compound which diminishes the absorbance of treated cells by 50% compared to untreated cells (10).

Genes expression profile

Following treatment of HT-29 cells for 48 hours with dichloromethane *Dorema ammoniacum* gum resin extract (IC_{50} concentration), total RNA was extracted from treated and controlled cells. After quantitative and qualitative measurements of the samples, the samples with an optical absorption ratio of 260/280 nm between 1.8-2 were used for

[DOI: 10.61186/rbmb.12.1.127]

cDNA synthesis. One microliter of extracted RNA was used using a 2-step PCR-RT kit and dT oligomer primers. The primers were designed using Gene Runner software, and the Blast program at the NCBI website checked the off-target sequence(s). Expressions of *APC (Gene ID 324), KRAS* (Gene ID 3845), and *P53* (Gene ID 7157) genes were performed by quantitative real-time PCR analysis, and the *GAPDH* (Gene ID 257) *gene* was used as a normalizer (Table 1). All reactions were examined by melting curve analysis. PCR reaction efficiency for all genes was analyzed before using relevant primers and constructing the standard curves (data not shown). The analysis of Real-time PCR data was performed using the 2-ΔΔCt method. The data were obtained from 3 separate experiments and presented as mean ± standard deviation (Mean ± SD). The mean difference was considered significant at the level of $*P< 0.05$, $** P< 0.01$ (11).

Table 1. List of primers, nucleotide sequence, and a melting point of primers.

Gene	Gene ID	Forward 5` to 3`	Reverse 5` to 3`	Tm	
				Forward	Reverse
P53	7157	GCCCAACAACACCAGCTCCT	CCTGGGCATCCTTGAGTTCC	56	56
KRAS	3845	CTATTCGCAGCTCACACAGTTTAC	TTCTTAATTTGGTCTGCGGC	54	54
APC	324	GACTGGTATTACGCTCAACTTCA	CAATTGCCTTCTGGTCATATCTG	56	56
GAPDH	257	AGGGCTGCTTTTAACTCTGG	CCCCACTTGATTTTGGAGGG	55	55

Metabolites extraction

HT-29 cells (8×10^6 cells) treated with IC_{50} concentration of dichloromethane extract except for control cultures. After incubation at 37 ºC for 48 hours, the cells were centrifuged at 1800 G for 10 min at 4 ºC. Then pellets were harvested for the extraction process of metabolites for NMR spectroscopy. Cells were resuspended in DMEM medium, centrifuged at 1800 G for 10 min at 4 ºC, and washed twice with PBS. 1.0 ml of chilled chloroform and methanol (1: 2 ratio) followed by chloroform and water (1:1 ratio) was added to the cell suspension, vortexed, and sonicated for 5 min at 4 ºC followed by centrifugation at 16000 G at 4 ºC for 20 min. Two phases were obtained, the upper phase was hydrophilic, and the lower was lipophilic. pH was adjusted to 6.8, and samples was lyophilized before NMR spectroscopy (12).

1HNMR spectroscopy

The lyophilized hydrophilic cell extracts (n=5) were resuspended in 600 μL of buffer (150 mM potassium phosphate at pH 7.4, 1 mM NaN3, and 0.01% trimethylsilyl propionate (TSP) (Sigma, CA, USA) as a chemical shift reference (δ=0 ppm) and imidazole (2 mM) in 100% D_2O and 600 μL deuterated chloroform was added to the lipophilic cell extracts (n=5). Samples were centrifuged, and 500 µl of the extracted samples were transferred into an NMR tube and analyzed on a Bruker AV-500 NMR spectrometer with field gradient operating at 500.13 MHz for proton observation at 298.6 K. One-dimensional 1HNMR spectra were recorded using a 10-µs pulse, 0.1 s mixing time, 3.0 s relaxation delay, 6410.6 Hz spectra width, and 500 scans with standard 1D NOESY pulse sequence to suppress the residual water peak (13).

Statistical analysis

The spectra obtained from the NMR spectrometer were preprocessed by ProMetab (v.3-3) function file written by Dr. Mark R. Viant, the University of Birmingham, in a Matlab (ver. R2020) environment. All spectra were Fourier transformed, phase and baseline corrected, and binned for 0.005 ppm, followed by the removal of the water peak at 4.7 ppm. The refined spectra were converted to multivariate metrics with Pareto scaling and normalization for further classification analysis by partial least square discrimination

[DOI: 10.61186/rbmb.12.1.127]

analysis (PLS-DA) methods. Chemical shift outliers were ascertained, and the corresponding metabolites were cited from the human metabolites database (HMDB). By applying the defined metabolites, identical pathways were also worked out by implementing the online Metaboanalyst metabolomics analysis software (v.5). Student's t-test was applied for gene expression and MTT assay.

Results

Cell viability

Evaluation of toxicity, susceptibility, and viability of different extracts of *Dorema ammoniacum* gum on HT-29 cells over 48 hours using the MTT method is shown in Figure 1 and Table 2 compared with controls. Our data reveal that chloroform, hexane, and dichloromethane extracts had the highest cytotoxic effect on HT-29 cells in 48 hours. The survival rate of HT-29 cells at 500 and 600 µg/ml concentration for hexane and dichloromethane was 0%, and chloroform extract at 500 and 600 µg/ml growth inhibition rate was 3.41% and 11.01%, respectively. The IC_{50} for the solvent components of *Dorema* ammoniacum gum is given in Table 2, with the lowest value for the chloroform solvent and then the hexane solvent. Dichloromethane solvent was the highest relative to the chloroform and hexane extraction.

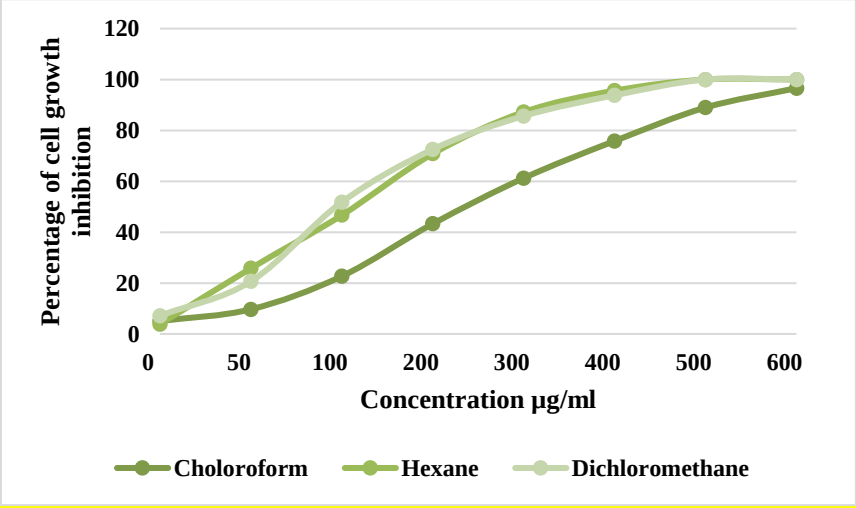

Fig. 1. The effect of chloroform, hexane, and dichloromethane extracts of *Dorema ammoniacum* gum after 24 hours of treatment on inhibition of HT-29 cell growth. As the dose of extracts increases, the rate of inhibition of cell proliferation also increases. Therefore, inhibition of cell proliferation by these extracts is dose dependent. All tests were performed with three replications, and data analysis was reported based on mean ± standard deviation.

Table 2. Percentage of cell viability and IC50 determined for different solvent components of *Dorema ammoniacum* gum.

Concentration (µg/ml)	Cell viability (%) ±SD		
	Chloroform Solvent	Hexane Solvent	Dichloromethane Solvent
0	94.71+8.25	96.17+10.05	82.24+6.44
50	90.30+7.65	74.18+6.87	79.30+1.82
100	77.30+8.06	53.31+4.69	48.16+3.91
200	46.07+2.74	29 16+3.08	27.44+3.10
300	38.75+2.58	12.79+1.05	14.33+1.23
400	24.16+1.52	4.37+0.53	6.19+0.53
500	11.01+0.85	0	0
600	3.41+0.26	0	0
IC50	243.8	124.12	114.81

Results were reported as cell viability percentages±SD as compared to untreated control samples.

[DOI: 10.61186/rbmb.12.1.127]

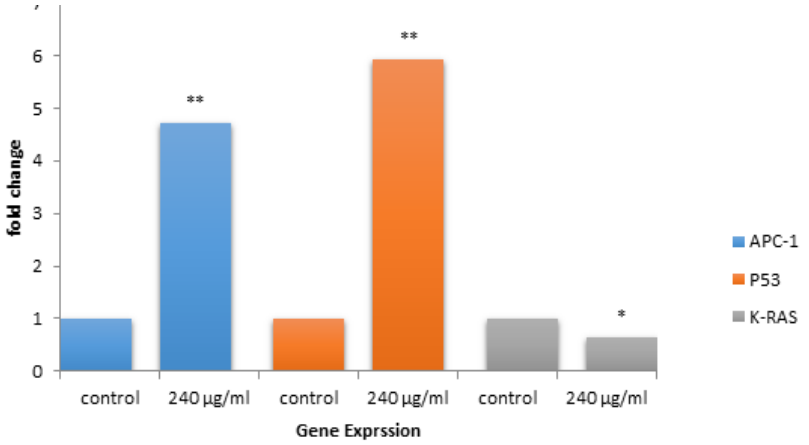

Fig. 2. Expression analysis by Real-time PCR method of *APC*, *KRAS*, and P53 genes in HT-29 class colorectal cancer cells after treatment with IC_{50} concentration of dichloromethane extract of *Dorema ammoniacum gum*. Data are expressed as mean ± SD in three independent experiments. (*P< 0.05, **P< 0.01).

Table 3. Results of integrated analysis of lipophilic and hydrophilic metabolites and potential *p53*, *APC*, and *KRAS* genes. Total, the total number of compounds in the pathway; Hits, the actual matched number from the user uploaded data; Raw p, the original p-value calculated from the enrichment analysis, using MetaboAnalyst database and changes in gene expression is gene fold changes with that of control.

Metabolic pathway	Participating Metabolites	Total	Hits	Pathway impact value	Raw p	Change in gene expression		
						APC	*P53*	*KRAS*
						4.72	4.92	2.23
						fold>+	fold>+	fold<-
Aminoacyl-tRNA biosynthesis	L-Glutamate L-Valine L-Isoleucine L-Lysine	74	4	0.054795	0.0021392	✓	✓	_
Nitrogen metabolism	L-Glutamate L-Glutamine	10	2	0.33333	0.0024915	_	✓	_
D-Glutamine and D-glutamate metabolism	L-Glutamate L-Glutamine	10	2	0.44444	0.0024915		✓	✓
Valine, leucine, and isoleucine biosynthesis	L-Isoleucine L-Valine	12	2	0.18182	0.0036204	✓		✓
Alanine, aspartate and glutamate metabolism	D-Aspartate L-Glutamate L-Glutamine	61	3	0.21667	0.010833	_	✓	✓
Arginine biosynthesis	L-Glutamate L-Glutamine	27	2	0.26923	0.01796	_	✓	_
Glycerolipid metabolism	Phosphatidate Triacylglycerol	35	2	0.20588	0.029341	_	✓	_
Purine metabolism	L-Glutamine dGTP Deoxyguanosine dGMP	166	4	0.10909	0.035799		✓	✓
Galactose metabolism	Alpha-D- Glucose D-Glucose	51	2	0.22	0.05841	✓	✓	✓
Glyoxylate and dicarboxylate metabolism	L-Glutamate L-Glutamine	56	2	0.036364	0.06895	_	✓	_

[DOI: 10.61186/rbmb.12.1.127]

Genes expression profiles

Based on the data obtained from the MTT assay, a concentration of IC_{50} (114.81µg/ml) of the dichloromethane extract of *Dorema ammoniacum* gum was used to treat HT-29 cells to assess changes in the expression profile of *APC*, *KRAS*, and *P53* genes. As shown in Figure 2, The analysis of real-time PCR data on gene expression showed that treatment with IC_{50} dichloromethane caused a significant increase in *p53* and *APC*-1 genes by approximately 5.92-fold and 4.72 –fold, respectively, compared to the control groups. However, the *KRAS* oncogene gene expression change was insignificant (0.64 -fold compared to untreated cells).

Metabolome profile

Table 3 describes the effect of pathways and their p values, the essential metabolites participating in each pathway, and convergent genes under the influence of treatment with dichloromethane solvent of *Dorema ammoniacum* gum.

Discussion

Treating HT-29 cells with dichloromethane extract of *Dorema ammoniacum* gum significantly increased the expression of *APC* and *p53* tumor suppressor genes and decreased the *KRAS* oncogene gene. Aminoacyl tRNA synthase abnormal expression, cellular localization, and molecular interactions induce various human diseases (14, 15). The earlier investigation revealed that the aminoacyl-tRNA biosynthesis pathway is upregulated in gastrointestinal cancer based on the integrated analysis of the metabolome and transcriptome of gastrointestinal cancer. The upregulated expression of TARS and FARSB, the key enzymes in the aminoacyl-tRNA biosynthesis pathway, was correlated with tumor metastasis and proliferation in gastrointestinal cancer (16). Analogously, Nam et al. showed that lysyl-tRNA synthetase played a vital role in the invasive dissemination of colon cancer spheroids in 3D collagen I gels (17). Moreover, certain Aminoacyl-tRNA synthetases and ARS-interacting multifunctional proteins could regulate tumorigenesis by p53 (18, 19). High-fat diet-induced colonic lysine homocysteinylation through MRS led to the accumulation of DNA damage and colorectal cancer-like phenotypes in the colon of mice and rats (19). Zhong et al. observed that IARS2 was highly expressed in human colon cancer tissues, and the knockdown of IARS2 could inhibit RKO cell proliferation, suggesting that IARS2 might trigger the development of colon cancer (20). Our investigation also reveals that this pathway altered along with p53 genes after the treatment.

The second altered pathway is nitrogen metabolism, which is particularly important in synthesizing nucleic acids, especially in anabolic processes. The most crucial nitrogen donor is glutamine. It enters the Krebs cycle through the anaplerotic pathway and is controlled by two enzymes, glutaminase (GLS1) and phosphoribosyl pyrophosphate amidotransferase (PPAT). An imbalance in these two enzymes increases tumorigenesis and cancer cell growth, so reducing the PPAT/GLS1 ratio in drug interventions disrupts the carcinogenic process (21, 22). Malignant cells rely on the amino acid glutamine as an anaplerotic substance and the most abundant amino acid due to their high need for energy and food sources for growth and proliferation and their strong dependence on glucose. Therefore, the metabolic pathway of glutamine and glutamate is cancer's most important known pathway. The *KRAS* oncogene gene in a PDCA mouse model regulates a metabolic pathway that supports glutamine for the growth and proliferation of pancreatic cancer cells (23, 24). In pancreatic cancer cells, a mutation in the *KRAS* gene causes the use of glutamine-derived aspartate, which, after being transferred to the cytoplasm by the aspartate transaminase GOT1 to oxaloacetate, then to malate and finally pyruvate, preserves the redox potential. However, glioma and neuroblastoma cancer cells enter the Krebs cycle by converting

[DOI: 10.61186/rbmb.12.1.127]

glutamate-derived glutamate by GLUD1 to alpha-ketoglutarate. Significant changes in glutamine metabolism and enzymes and proteins involved in glutamine metabolism were observed in colorectal cancer cells with *KRAS* or BRAF mutations (23, 24). On the other hand, the *p53* gene increases glutaminase 2 (GLS2) expression by accelerating glutamine conversion to glutamate and supports anaplerosis in cancer cells (25, 26). The process of oncogenesis in cancer cells due to metabolic flexibility and the glycolysis pathway requires metabolites and other alternative pathways, such as using amino acids as building blocks of proteins and precursors of nucleic acids and energy sources of branched-chain amino acids (25, 26).

The *KRAS* oncogene gene directs the metabolism of branched-chain amino acids in pancreatic cancer (PDAC) and Non-small-cell lung carcinoma (NSCLC) by regulating BCAT2 expression. On the other hand, the *KRAS* gene plays a vital role in regulating nutrient metabolism. The high level of branched-chain amino acids in the blood of patients with pancreatic cancer, especially in the early stages, shows the critical role of this gene in protein breakdown and metabolism of branched-chain amino acids. The second irreversible step is the branched-chain α-keto acid dehydrogenase (BCKDH) enzyme complex, which increases tumorigenesis in colorectal cancer through the MEK-ERK signaling pathway, especially in metastatic colorectal cancer (27-29).

Metabolism of alanine, aspartate, glutamate, and arginine biosynthesis are other pathways that have been altered by treatment with the dichloromethane extract of *Dorema ammoniacum* gum. The amino acid aspartate is a non-essential amino acid recharged by the enzyme L-asparaginase from the breakdown of the amino acid asparagine in the cell. However, proliferation can be increased in certain conditions and cancer cells by directing aspartate to nucleic acid biosynthesis. By inhibiting the synthesis of asparagine synthase, the *p53* gene causes the accumulation of aspartate in lymphoma and colorectal cancer cells, activating the LKB1-AMPK signaling pathway, which ultimately inhibits the cell cycle (30). Mutations and disruption of the *p53* gene in cancer cells cause abnormal proliferation in these cells (31). In Non-small-cell lung carcinoma (NSCLC), glutamine deficiency modulates *KRAS* gene expression and activates the *KRAS-Akt-Nrf2-ATF4* pathway, which induces ATF4 and increases ASNS expression, maintaining cell survival and inhibiting apoptosis. Although the data analysis predicted more pathways for us with the Metaboanalyst software, the most critical convergent pathway with the gene was examined according to the p-values (32).

We demonstrated the cytotoxicity of different extracts of *Dorema ammoniacum* gum against HT-29 cells. The dichloromethane extract of *Dorema ammoniacum* gum affected the expression of genes affecting *APC* HT-29 cell; *p53* and *KRAS* disrupted metabolic flexibility in these cells and reduced the oncogenesis process in these cells. However, to increase the validity of this research, it is necessary to investigate the effect of compounds fraction derived from *Dorema ammoniacum* gum on biological activities, particularly the anti-carcinogenic properties and related signaling pathways.

Acknowledgement

The authors would like to thanks Dr. Zahra Zamani, Pasteur Institute of Iran for her kind help during the experiments.

Funding

This work is a part of PhD Student, and no financial support was received.

Conflict of Interest

The authors have no conflict of interest to declare.

[DOI: 10.61186/rbmb.12.1.127]

References

1. Bray F, Ferlay J, Soerjomataram I, Siegel RL, Torre LA, Jemal A. Global cancer statistics 2018: GLOBOCAN estimates of incidence and mortality worldwide for 36 cancers in 185 countries. CA Cancer J Clin. 2018;68(6):394-424.
2. Bayatiani MR, Ahmadi A, Aghabozorgi R, Seif F. Concomitant Up-Regulation of Hsa- Mir-374 and Down-Regulation of Its Targets, GSK-3beta and APC, in Tissue Samples of Colorectal Cancer. Rep Biochem Mol Biol. 2021;9(4):408-16.
3. Chen HJ, Wei Z, Sun J, Bhattacharya A, Savage DJ, Serda R, et al. A recellularized human colon model identifies cancer driver genes. Nat Biotechnol. 2016;34(8):845-51.
4. Cancer Genome Atlas N. Comprehensive molecular characterization of human colon and rectal cancer. Nature. 2012;487(7407):330-7.
5. Bakhtiarian A, Shojaii A, Hashemi S, Nikoui V. Evaluation of Analgesic and Anti-Inflammatory Activity of Dorema Ammoniacum Gum in Animal Model. Int J Pharm Sci Res. 2017;8(7):3102-6.
6. Mazaheritehrani M, Hosseinzadeh R, Mohadjerani M, Tajbakhsh M, Ebrahimi SN. Acetylcholinesterase Inhibitory Activity of Dorema Ammoniacum Gum Extracts and Molecular Docking Studies. Int J Pharm Sci Res. 2020;11(2):637-44.
7. Adhami HR, Lutz J, Kählig H, Zehl M, Krenn L. Compounds from gum ammoniacum with acetylcholinesterase inhibitory activity. Sci Pharm. 2013;81(3):793-805.
8. Ramola B, Kumar V, Nanda M, Mishra Y, Tyagi T, Gupta A, Sharma N. Evaluation, comparison of different solvent extraction, cell disruption methods and hydrothermal liquefaction of Oedogonium macroalgae for biofuel production. Biotechnol Rep (Amst). 2019;22:e00340.
9. Chahardehi AM, Arsad H, Ismail NZ, Lim V. Low cytotoxicity, and antiproliferative activity on cancer cells, of the plant Senna alata (Fabaceae). Rev De Biol Trop. 2021;69(1):317-30.
10. Mosmann T. Rapid colorimetric assay for cellular growth and survival: application to proliferation and cytotoxicity assays. J Immunol Methods. 1983;65(1-2):55-63.
11. Raeisossadati R, Abbaszadegan MR, Moghbeli M, Tavassoli A, Kihara AH, Forghanifard MM. Aberrant expression of DPPA2 and HIWI genes in colorectal cancer and their impacts on poor prognosis. Tumour Biol. 2014;35(6):5299-305.
12. Lodi A, Ronen SM. Magnetic resonance spectroscopy detectable metabolomic fingerprint of response to antineoplastic treatment. PLoS One. 2011;6(10):e26155.
13. Ahmadi M, Akhbari Z, Zamani Z, Hajhossieni R, Arjmand M. Study the Mechanism of Antileishmanial Action of Xanthium strumarium Against Amastigotes Stages in Leishmania major: A Metabolomics Approach. Jundishapur J Nat Pharm Prod. 2021;16(3).
14. Park SG, Schimmel P, Kim S. Aminoacyl tRNA synthetases and their connections to disease. Proc Natl Acad Sci USA. 2008;105(32):11043-9.
15. D'Hulst G, Soro-Arnaiz I, Masschelein E, Veys K, Fitzgerald G, Smeuninx B, et al. PHD1 controls muscle mTORC1 in a hydroxylation-independent manner by stabilizing leucyl tRNA synthetase. Nat commun. 2020;11(1):174.
16. Zhou Z, Sun B, Huang SQ, Yu DS, Zhang XC. Roles of aminoacyl-tRNA synthetase-interacting multi-functional proteins in physiology and cancer. Cell Death Dis. 2020;11(7):579.
17. Nam SH, Kim D, Lee M-S, Lee D, Kwak TK, Kang M, et al. Noncanonical roles of membranous lysyl-tRNA synthetase in transducing cell-substrate signaling for invasive dissemination of colon cancer spheroids in 3D collagen I gels. Oncotarget. 2015;6(25):21655-74.
18. Park B-J, Kang JW, Lee SW, Choi S-J, Shin YK, Ahn YH, et al. The haploinsufficient tumor suppressor p18 upregulates p53 via interactions with ATM/ATR. Cell. 2005;120(2):209-21.
19. Wang ZP, Tian Y, Lin J. Role of wild-type p53-induced phosphatase 1 in cancer. Oncol Lett. 2017;14(4):3893-8.
20. Zhong L, Zhang Y, Yang J-Y, Xiong L-F, Shen T, Sa YL, et al. Expression of IARS2 gene in colon cancer and effect of its knockdown on

[DOI: 10.61186/rbmb.12.1.127]

biological behavior of RKO cells. Int J Clin Exp Pathol. 2015;8(10):12151-9.
21. Kurmi K, Haigis MC. Nitrogen Metabolism in Cancer and Immunity. Trends Cell Biol. 2020;30(5):408-24.
22. Li L, Mao Y, Zhao L, Li L, Wu J, Zhao M, et al. p53 regulation of ammonia metabolism through urea cycle controls polyamine biosynthesis. Nature. 2019;567(7747):253-6.
23. Toda K, Kawada K, Iwamoto M, Inamoto S, Sasazuki T, Shirasawa S, et al. Metabolic Alterations Caused by KRAS Mutations in Colorectal Cancer Contribute to Cell Adaptation to Glutamine Depletion by Upregulation of Asparagine Synthetase. Neoplasia. 2016;18(11):654-65.
24. Hutton JE, Wang X, Zimmerman LJ, Slebos RJ, Trenary IA, Young JD, et al. Oncogenic KRAS and BRAF Drive Metabolic Reprogramming in Colorectal Cancer. Mol Cell Proteomics. 2016;15(9):2924-38.
25. Suzuki S, Tanaka T, Poyurovsky MV, Nagano H, Mayama T, Ohkubo S, et al. Phosphate-activated glutaminase (GLS2), a p53-inducible regulator of glutamine metabolism and reactive oxygen species. Proc Natl Acad Sci USA. 2010;107(16):7461-6.
26. Brown RE, Short SP, Williams CS. Colorectal Cancer and Metabolism. Curr Colorectal Cancer Rep. 2018;14(6):226-41.
27. Xue P, Zeng F, Duan Q, Xiao J, Liu L, Yuan P, et al. BCKDK of BCAA Catabolism Cross-talking With the MAPK Pathway Promotes Tumorigenesis of Colorectal Cancer. EBioMedicine. 2017;20:50-60.
28. Tian Q, Yuan P, Quan C, Li M, Xiao J, Zhang L, et al. Phosphorylation of BCKDK of BCAA catabolism at Y246 by Src promotes metastasis of colorectal cancer. Oncogene. 2020;39(20):3980-96.
29. Yoshie T, Nishiumi S, Izumi Y, Sakai A, Inoue J, Azuma T, Yoshida M. Regulation of the metabolite profile by an APC gene mutation in colorectal cancer. Cancer Sci. 2012;103(6):1010-21.
30. Makia R, Al-Sammarrae K, Al-Halbosiy M, Al-Mashhadani M. In Vitro Cytotoxic Activity of Total Flavonoid from Equisetum Arvense Extract. Rep Biochem Mol Biol. 2022;11(3):487-92.
31. Deng L, Yao P, Li L, Ji F, Zhao S, Xu C, et al. p53- mediated control of aspartate- asparagine homeostasis dictates LKB1 activity and modulates cell survival. Nat Commun. 2020;11(1):1755.
32. Gwinn DM, Lee AG, Briones-Martin-Del-Campo M, Conn CS, Simpson DR, Scott AI, et al. Oncogenic KRAS Regulates Amino Acid Homeostasis and Asparagine Biosynthesis via ATF4 and Alters Sensitivity to L-Asparaginase. Cancer Cell. 2018;33(1):91-107 e6.

[DOI: 10.61186/rbmb.12.1.127]